Electronic Supplementary Material (ESI) for Journal of Materials Chemistry A.

Supplementary Information

for

Nanoporous $(Pt_{1-x}Fe_x)_3Al$ intermetallic compounds for much enhanced oxygen electroreduction catalysis

Tuo Cheng, Xing-You Lang,* Gao-Feng Han, Rui-Qi Yao, Zi Wen, Qing Jiang*

Key Laboratory of Automobile Materials (Jilin University), Ministry of Education, and School of Materials Science and Engineering, Jilin University, Changchun 130022, China

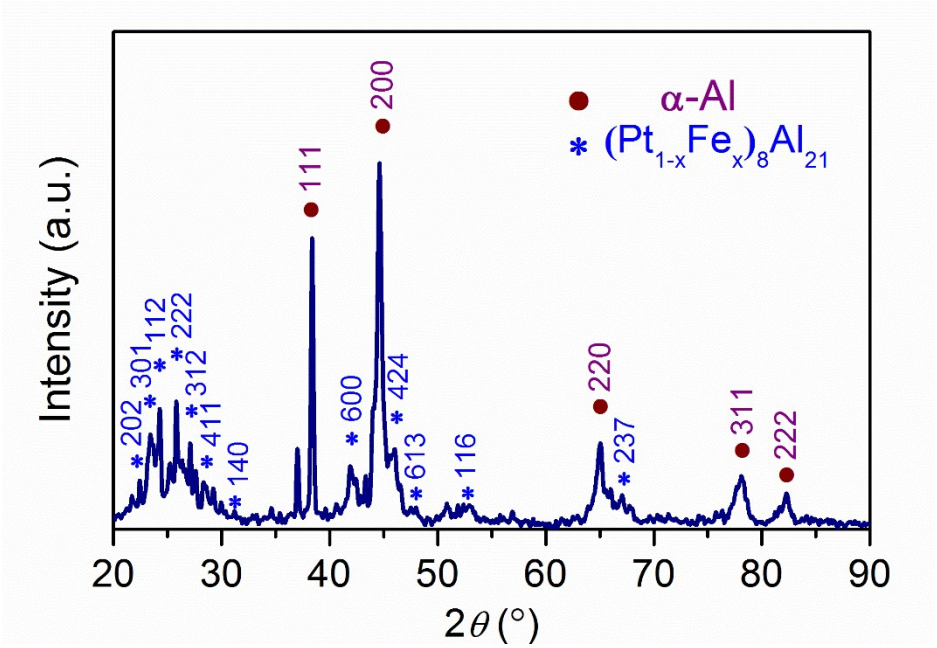

Figure S1. X-ray diffraction (XRD) pattern of precursor $Pt_{10}Fe_2Al_{88}$ alloy ribbons.

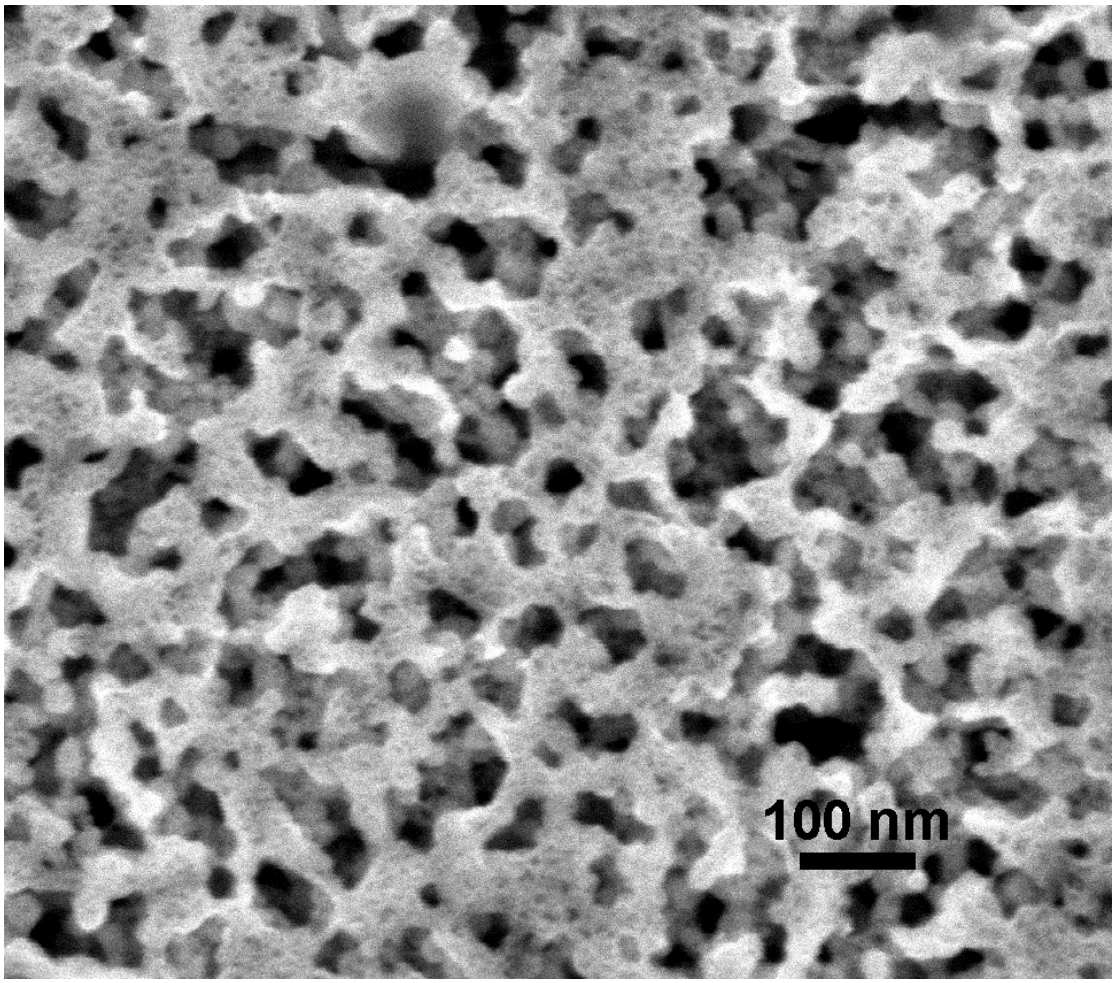

Figure S2. Typically top-view SEM image of the dealloyed NP $(Pt_{1-x}Fe_x)_3Al/Pt$.

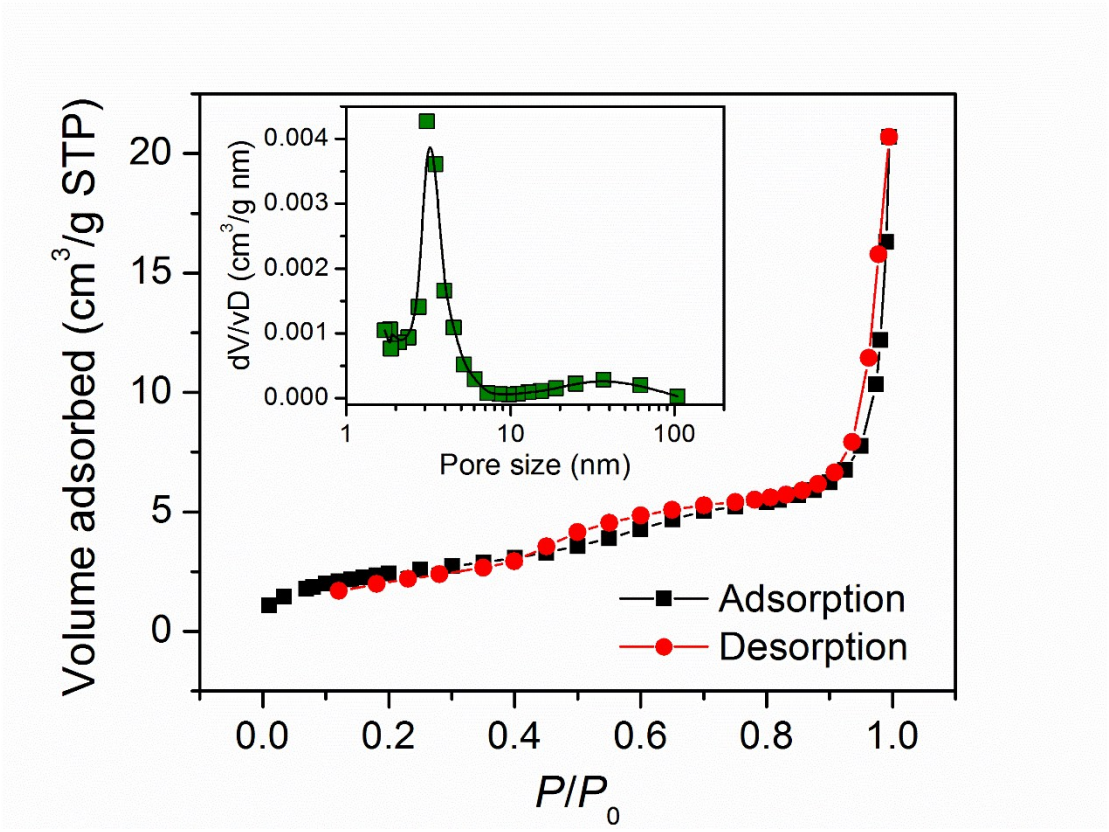

Figure S3. Nitrogen adsorption/desorption isotherm of NP $(Pt_{1-x}Fe_x)_3Al$/Pt. (Inset shows the pore size distribution.

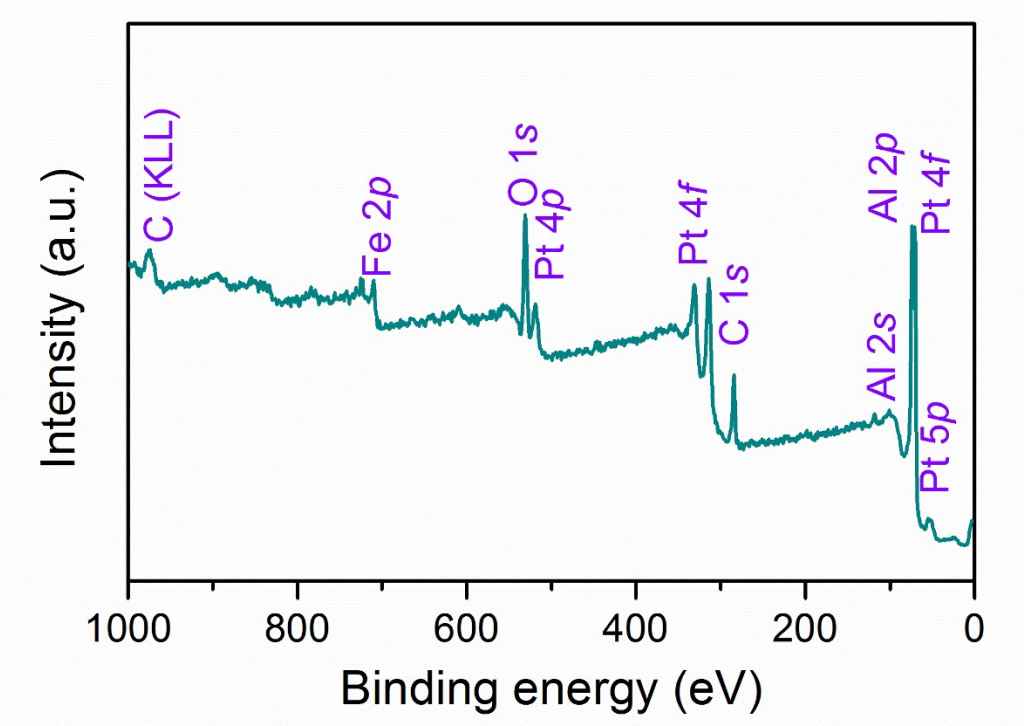

Figure S4. XPS survey spectrum for the as-dealloyed NP $(Pt_{1-x}Fe_x)_3Al/Pt$.

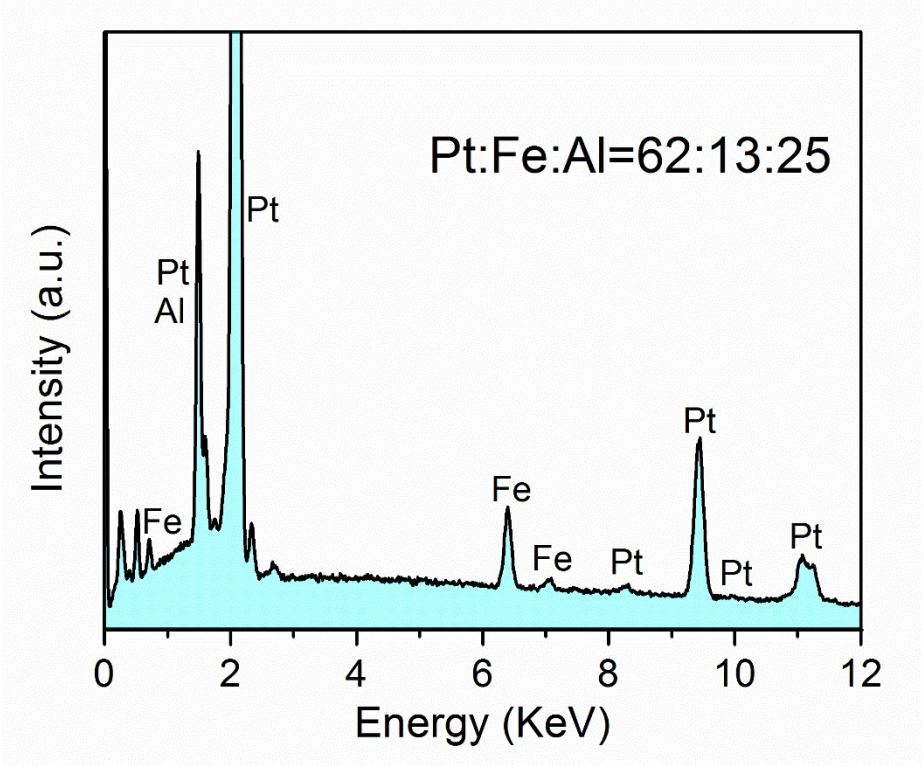

Figure S5. EDS of the as-dealloyed NP $(Pt_{1-x}Fe_x)_3Al$/Pt particles.

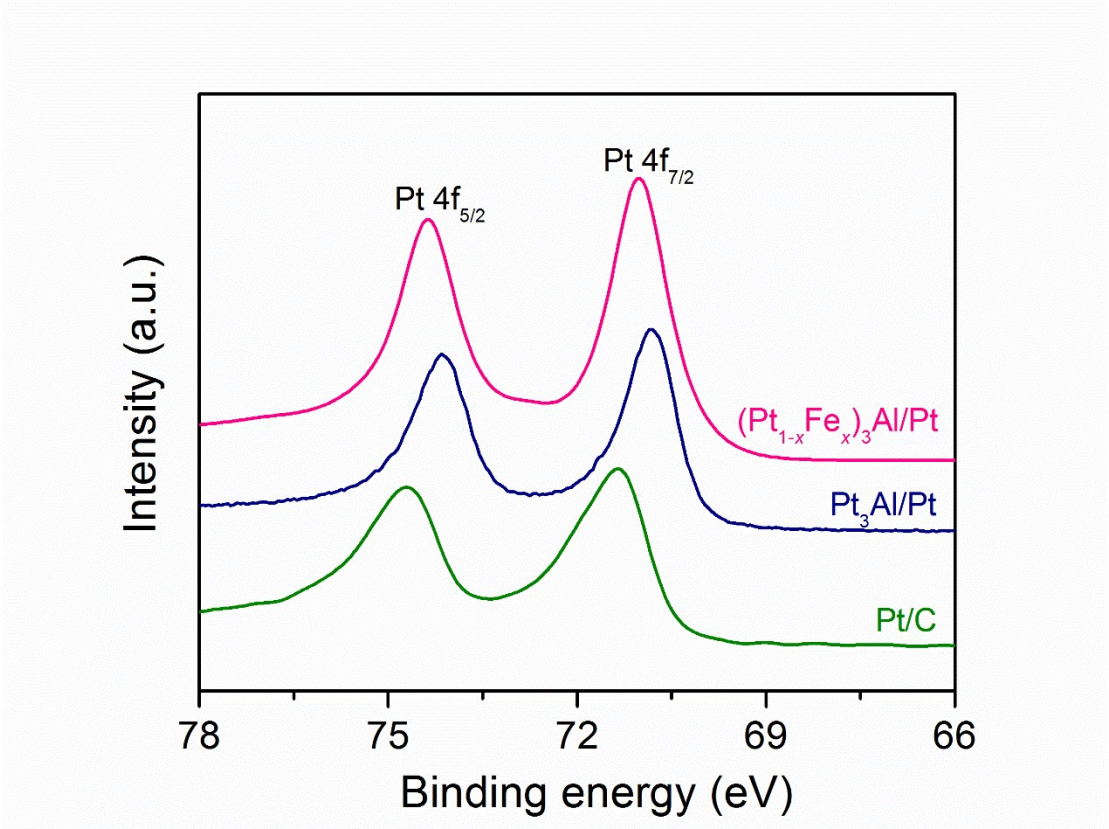

Figure S6. High-resolution XPS spectra of Pt 4*f* for NP $(Pt_{1-x}Fe_x)_3Al/Pt$, Pt_3Al/Pt and Pt/C nanocatalysts.

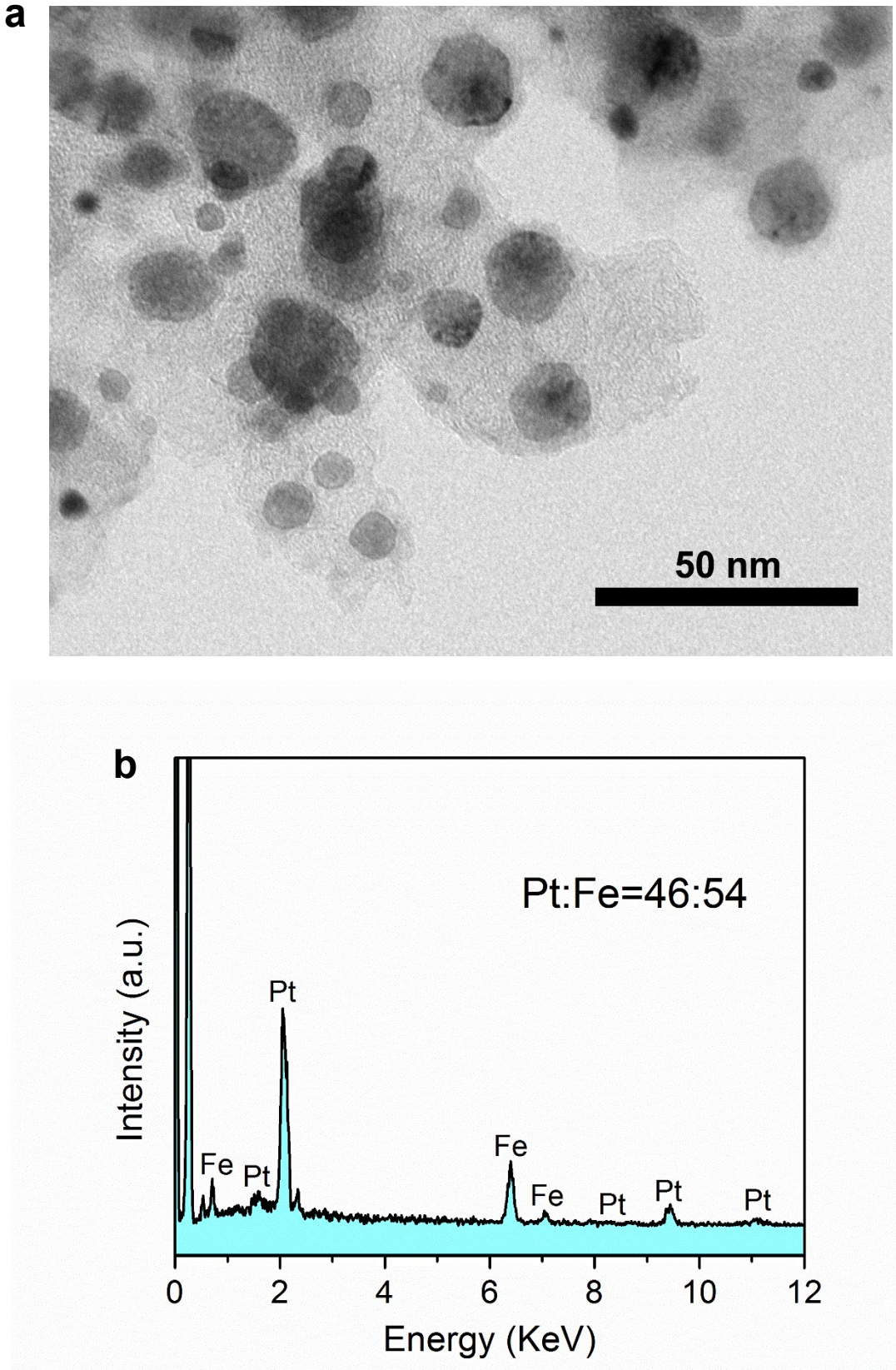

Figure S7. (**a**) TEM image and (**b**) EDS of NP $Pt_{46}Fe_{54}$/Pt/C particles, which are fabricated by dealloying $Pt_{28}Fe_{72}$/C precursor.

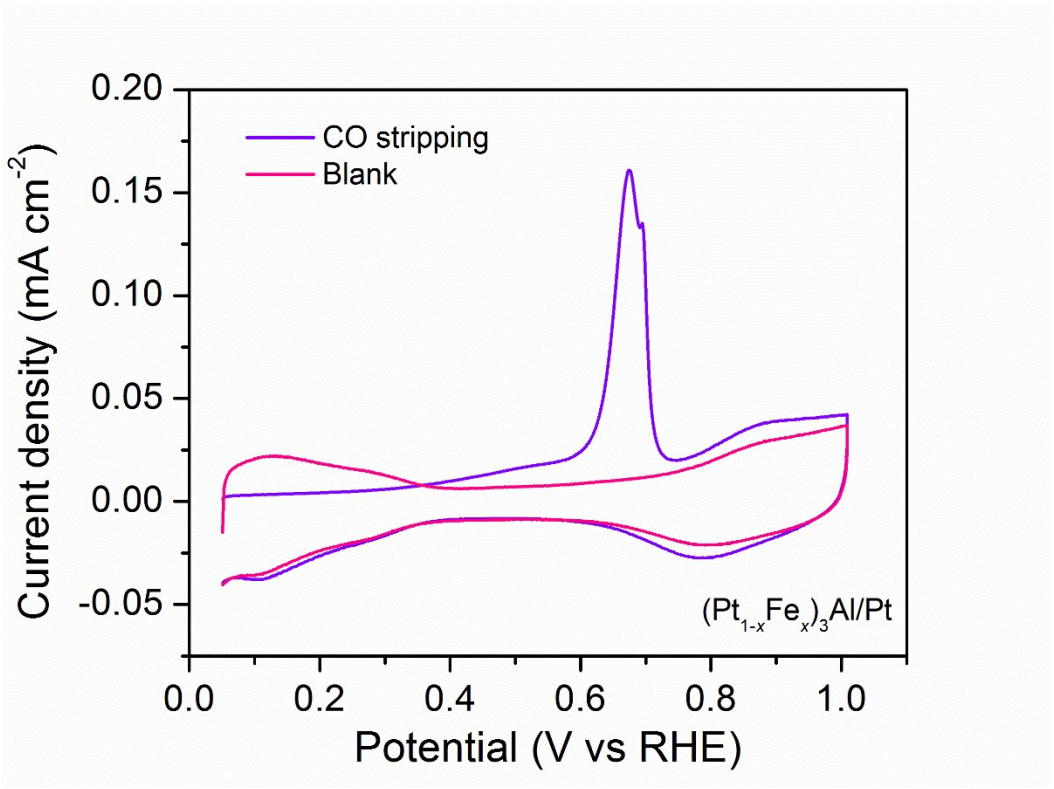

Figure S8. CV curves of $(Pt_{1-x}Fe_x)_3Al/Pt$ signifying the difference in surface coverage by H_{upd} and OH_{ad}. ECSA of the NP $(Pt_{1-x}Fe_x)_3Al/Pt$ are determined by integrated charge of adsorbed CO electro-oxidation curves.

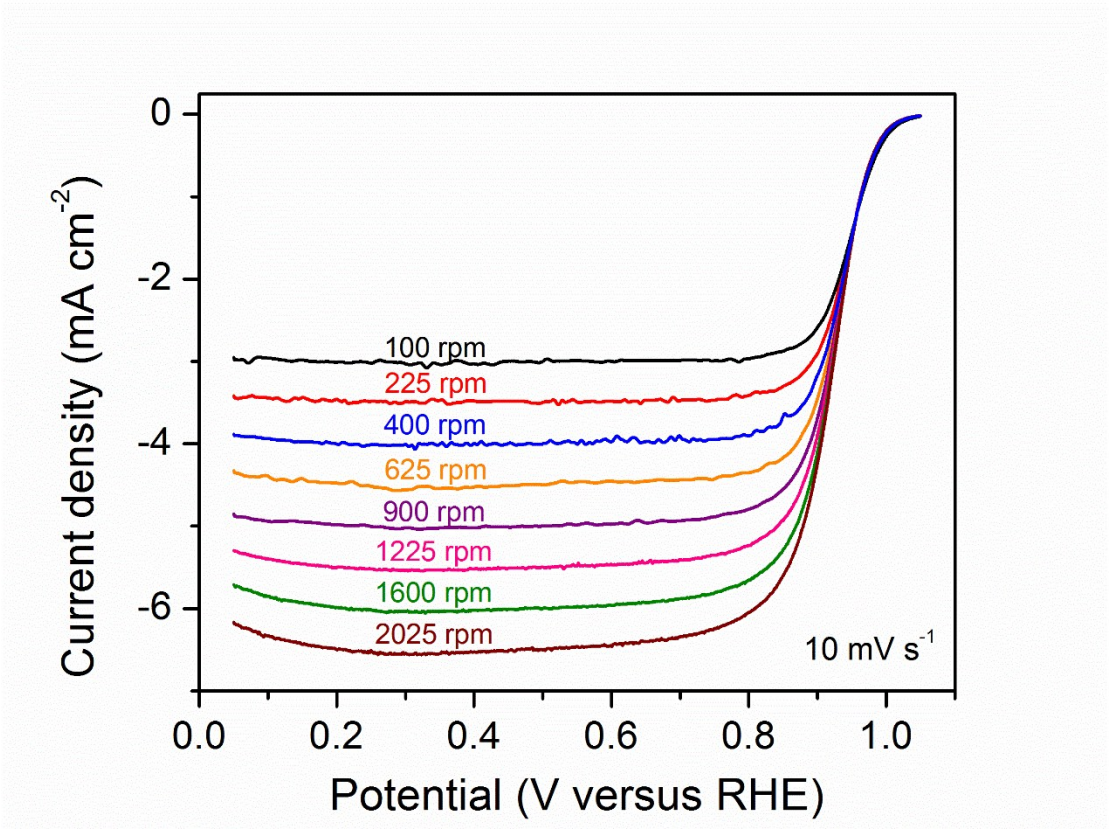

Figure S9. ORR polarization curves of NP $(Pt_{1-x}Fe_x)_3Al$/Pt in an O_2-saturated 0.1 M $HClO_4$ solutions at room temperature and a scan rate of 10 mV s^{-1} with different rotation speeds.

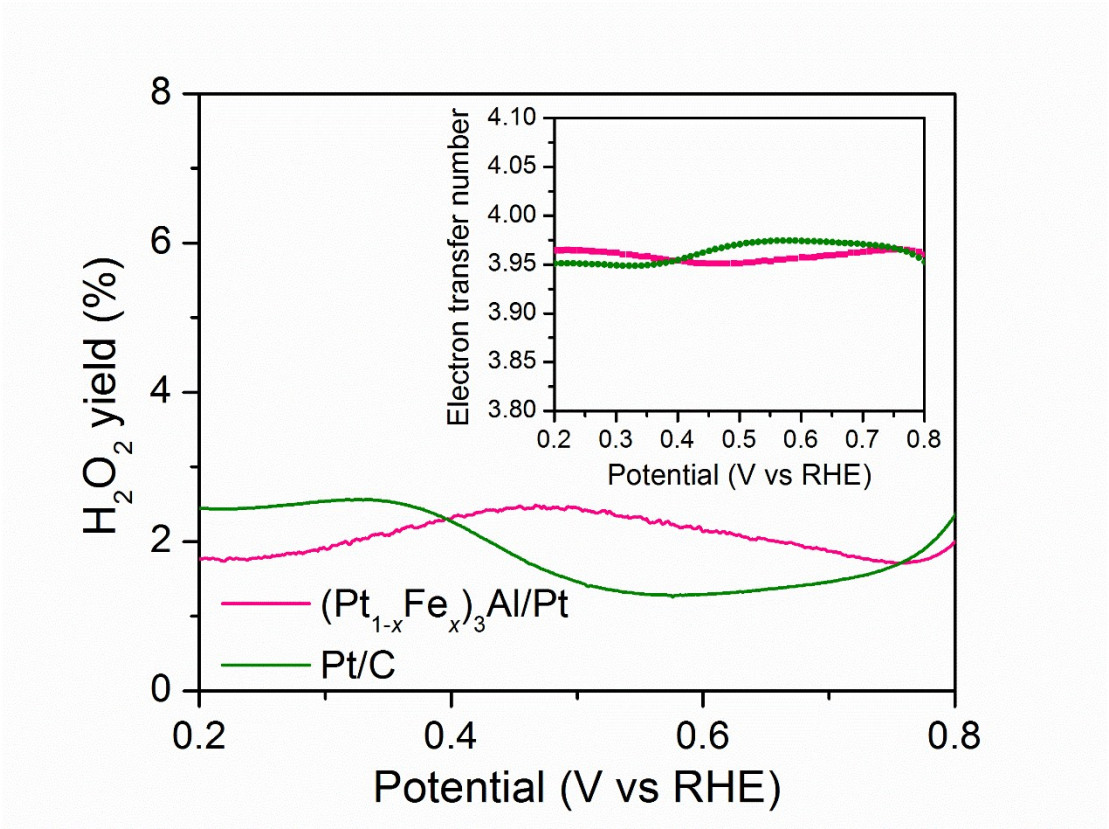

Figure S10. H_2O_2 yield of NP $(Pt_{1-x}Fe_x)_3Al/Pt$ and Pt/C catalyst. Inset: Electron transfer number as functions of the electrode potential.

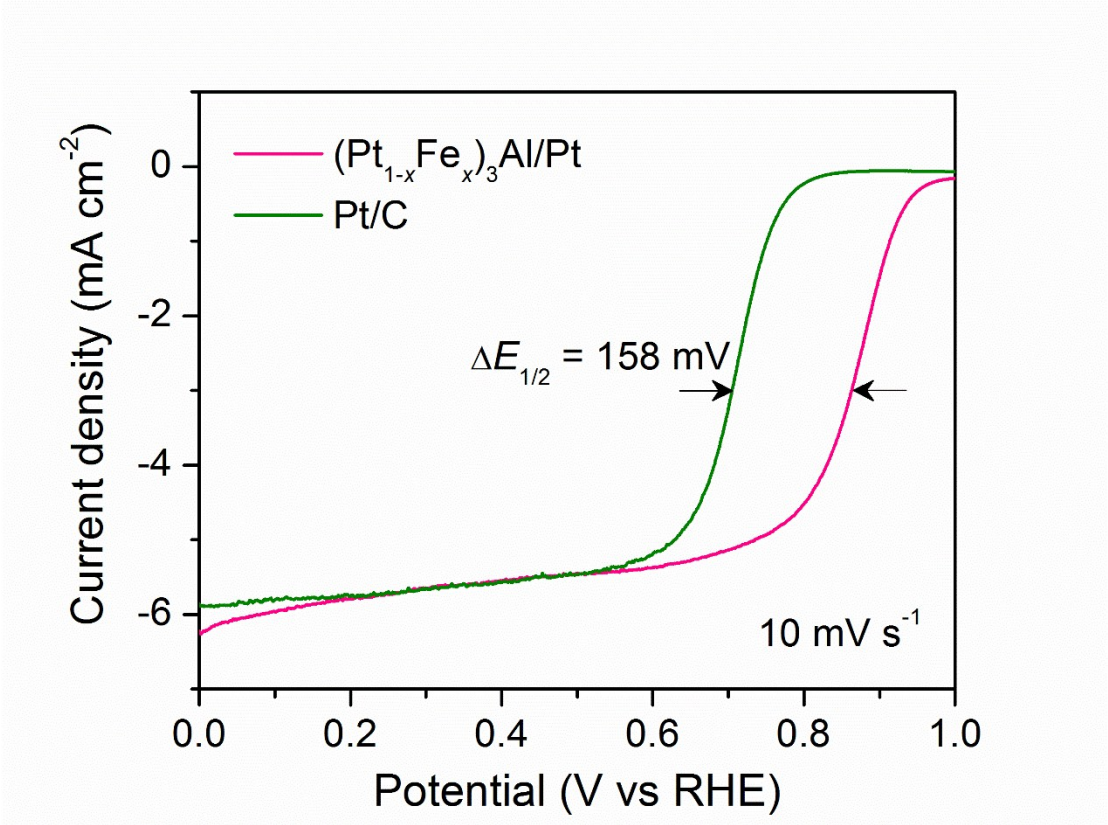

Figure S11. ORR polarization curves for NP $(Pt_{1-x}Fe_x)_3Al/Pt$ and Pt/C in O_2-purged 0.1 M KOH solution at room temperature with a scan rate of 10 mV s^{-1} and a rotation rate of 1600 r.p.m..

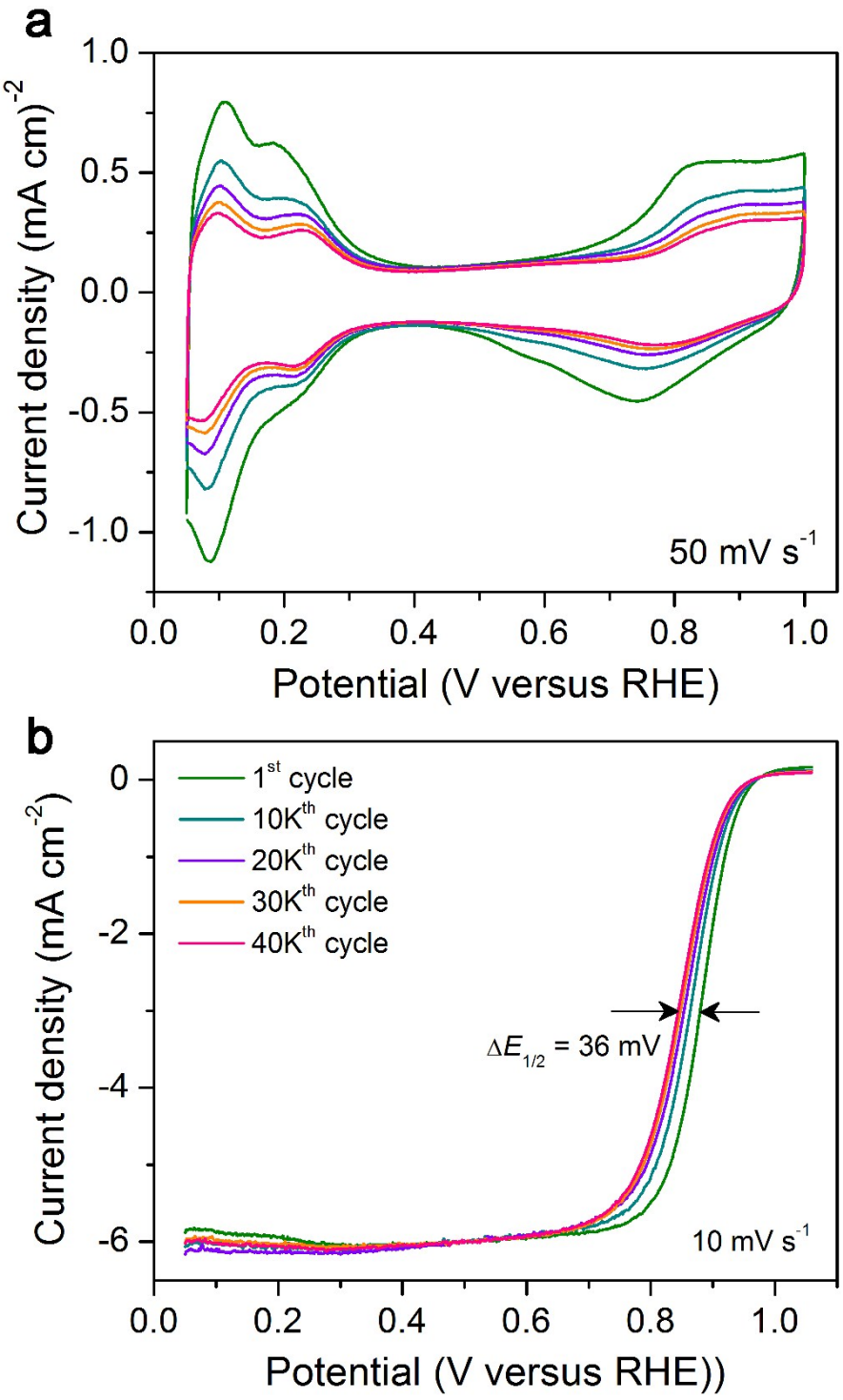

Figure S12. (**a**) CV curves for the 40,000-cycle stability test of Pt/C nanocatalyst in N_2-purged 0.1 M $HClO_4$ at 50 mV s^{-1} within a potential window of 0.6 to 1.0 V. (**b**) ORR polarization curves for the Pt/C nanocatalyst in a long-term cycling test of 40,000 potential cycles, collected in O_2-saturated 0.1 M $HClO_4$ aqueous electrolyte at room temperature with a rotation rate of 1600 r.m.p. and a scan rate of 10 mV s^{-1}.

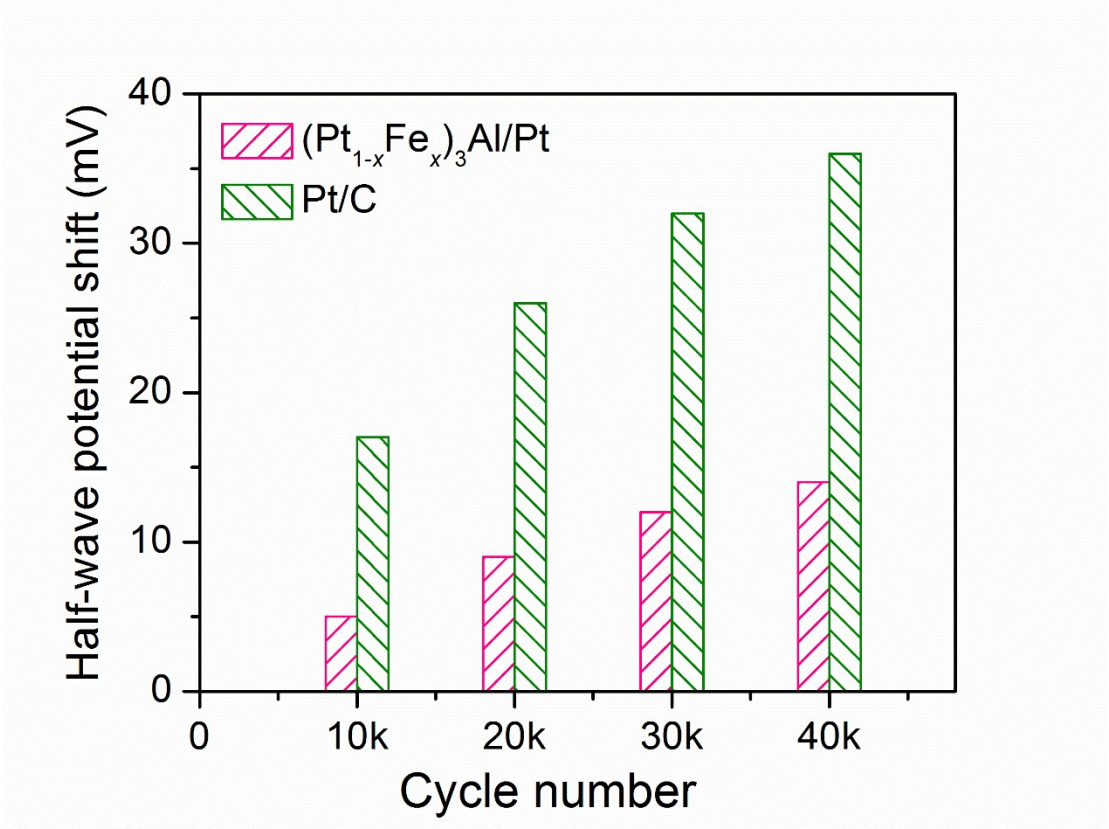

Figure S13. Evolution of half-wave potential for NP $(Pt_{1-x}Fe_x)_3Al/Pt$ and Pt/C nanocatalysts as a function of cycle number.

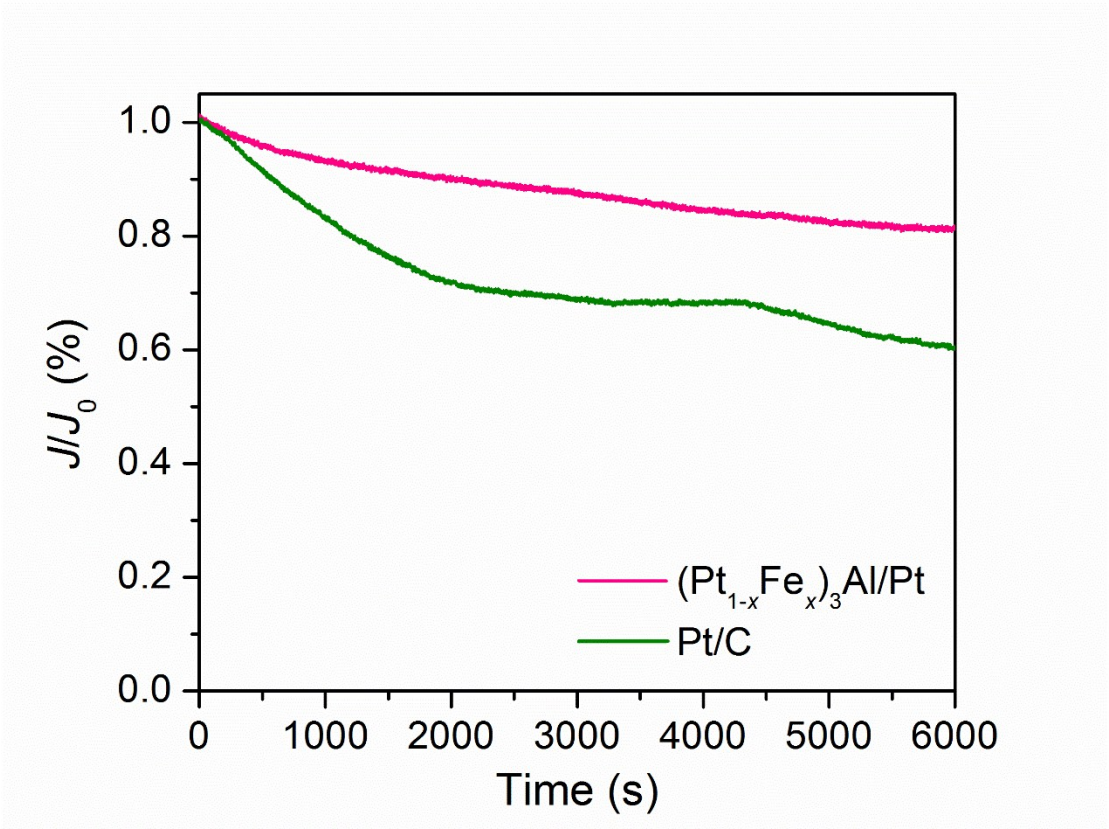

Figure S14. Normalized Current-time curves of NP $(Pt_{1-x}Fe_x)_3Al/Pt$ and Pt/C catalysts in O_2-saturated 0.1 M $HClO_4$ solution at 0.9 V.